

DO-TH 11/14

THE PHENO-ANALYSIS OF $B \rightarrow K^{(*)}\mu^+\mu^-$ DECAYS IN 2011 PLUS

G.HILLER

Institut für Physik, Technische Universität Dortmund, D-44221 Dortmund, Germany

We report on recent developments in the phenomenology of exclusive $b \rightarrow s\mu^+\mu^-$ decays in testing the standard model and explore its borders: the benefits of the region of large dimuon invariant masses and the exploitation of the angular distributions. Consequences of model-independent analyses from current and future data are pointed out.

1 Introduction

There exists a strong and long-standing interest in $\Delta B = 1$ exclusive $b \rightarrow s\mu^+\mu^-$ processes because of their accessibility at hadron colliders, good theory control and sensitivity to short-distance physics with and beyond the standard model, see, for instance^{1,2}. Many modes have been observed by now by several experiments with branching ratios at the level of $10^{-(6-7)}$, such as $B \rightarrow K^{(*)}\mu^+\mu^-$ by BaBar³, Belle⁴, CDF⁵, and recently $B_s \rightarrow \Phi\mu^+\mu^-$ decays by CDF⁵.

At present, each experiment has collected about order hundred events per mode. This already enables dedicated studies of spectra and asymmetries^{6,7}, which exhibit a much larger sensitivity to electroweak physics than the determination of the (un-binned integrated) branching ratios. The situation will further improve in the near future with the anticipated updates from the b -factories and the Tevatron, and with the ongoing run of the LHC. In fact, LHCb has reported 35 $B^+ \rightarrow K^+\mu^+\mu^-$ events in 37 pb^{-1} , and expects by the end of 2011 with 1 fb^{-1} order 10^3 $B \rightarrow K^*\mu^+\mu^-$ events⁸.

2 $B \rightarrow K^*\mu^+\mu^-$ Theory and Recent Highlights

The kinematically available phase space in $B \rightarrow K^{(*)}\mu^+\mu^-$ decays is $4m_\mu^2 \leq q^2 < (m_B - m_{K^{(*)}})^2$ for the dilepton invariant mass squared q^2 . This region is fully covered experimentally with the exception of the J/Ψ and Ψ' resonances from $B \rightarrow K^{(*)}(\bar{c}c) \rightarrow K^{(*)}\mu^+\mu^-$, which are removed by cuts. A systematic theory treatment exists for the region of high $q^2 \sim \mathcal{O}(m_b^2)$ by means of an operator product expansion (OPE) put forward by Grinstein and Pirjol some time ago⁹. The latter approach has recently been phenomenologically developed and exploited^{6,7}. We give a brief overview of the benefits of the high- q^2 region, corresponding to low hadronic recoil, in Section 2.1. In the region of low q^2 , where the $K^{(*)}$ is energetic in the B restframe, the decays are eligible to QCD factorization methods¹⁰. The region between the J/Ψ and the Ψ' peaks is informative on charmonia physics¹¹.

Because of the different theory frameworks applicable to the low- q^2 and high- q^2 region, as well as the resonance veto, appropriately q^2 -binned data are vital for precisely testing the standard model with exclusive semileptonic $b \rightarrow s\mu^+\mu^-$ modes. The current situation is exemplified in Figure 1 for the forward-backward asymmetry A_{FB} in $B \rightarrow K^*\mu^+\mu^-$ decays.

2.1 The High- q^2 Region

The OPE⁹ in $1/Q$, $Q = \{m_b, \sqrt{q^2}\}$ is combined with the improved heavy quark form factor relations¹² between the dipole form factors $T_{1,2,3}$ and vector ones $V, A_{1,2}$. To leading order in $1/m_b$ and including radiative corrections

$$T_1(q^2) = \kappa V(q^2), \quad T_2(q^2) = \kappa A_1(q^2), \quad T_3(q^2) = \kappa A_2(q^2) \frac{m_B^2}{q^2}, \quad (1)$$

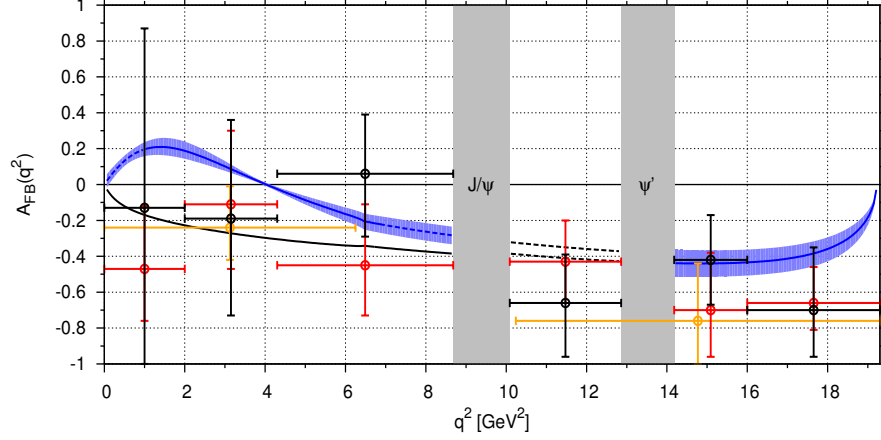


Figure 1: $A_{\text{FB}}(B \rightarrow K^* \mu^+ \mu^-)$ in the standard model (blue band) versus data: CDF '10 with 4.4fb^{-1} (black), BaBar '08 (gold) and Belle '09 (red). The black solid curve corresponds to $C_7 = -C_7^{\text{SM}}$. Figure taken from [6].

where $\kappa = 1 - 2\alpha_s/3\pi \ln(\mu/m_b) \simeq 1$. The heavy quark-based OPE is powerful because it predicts a simple transversity structure for the $B \rightarrow K^* \mu^+ \mu^-$ decay amplitudes: Each of the transversity amplitudes $A_i^{L/R}$, $i = 0, \perp, \parallel$ factorizes into universal short-distance $C^{L/R}$ and form factor coefficients f_i as^{6 a}

$$A_i^{L/R} \propto C^{L/R} \cdot f_i, \quad (2)$$

up to corrections of order $\alpha_s \Lambda/m_b$ and $(C_7/C_9)\Lambda/m_b$ that is, a few percent. This in turn allows to design high- q^2 observables which are^{6 7}

1. independent of the form factors ($H_T^{(2,3)}$, $a_{\text{CP}}^{(i)}$); note that $H_T^{(3)}$ probes the same short-distance physics as A_{FB} while having a significantly smaller theoretical uncertainty.
2. independent of the short-distance coefficients (f_i/f_j) and test the form factors at low recoil, for instance, the ratio $V/A_1 \propto \sqrt{(2J_2^s + J_3)/(2J_2^s - J_3)}$. An extraction from data can be used to compare against theory predictions from lattice²⁰ or other means.
3. independent of neither short-distance nor form factor coefficients and test the theoretical low recoil framework, such as

$$H_T^{(1)} = 1, \quad J_7 = 0. \quad (3)$$

The new form factor-free high- q^2 observables $H_T^{(i)}$ are defined in terms of the transversity amplitudes as

$$H_T^{(1)}(q^2) = \frac{\text{Re}(A_0^L A_{\parallel}^{L*} + A_0^{R*} A_{\parallel}^R)}{\sqrt{(|A_0^L|^2 + |A_0^R|^2)(|A_{\parallel}^L|^2 + |A_{\parallel}^R|^2)}} = \frac{\sqrt{2}J_4}{\sqrt{-J_2^c(2J_2^s - J_3)}}, \quad (4)$$

$$H_T^{(2)}(q^2) = \frac{\text{Re}(A_0^L A_{\perp}^{L*} - A_0^{R*} A_{\perp}^R)}{\sqrt{(|A_0^L|^2 + |A_0^R|^2)(|A_{\perp}^L|^2 + |A_{\perp}^R|^2)}} = \frac{\beta_l J_5}{\sqrt{-2J_2^c(2J_2^s + J_3)}}, \quad (5)$$

$$H_T^{(3)}(q^2) = \frac{\text{Re}(A_{\parallel}^L A_{\perp}^{L*} - A_{\parallel}^{R*} A_{\perp}^R)}{\sqrt{(|A_{\parallel}^L|^2 + |A_{\parallel}^R|^2)(|A_{\perp}^L|^2 + |A_{\perp}^R|^2)}} = \frac{\beta_l J_6}{2\sqrt{(2J_2^s)^2 - J_3^2}}, \quad (6)$$

or likewise the angular coefficients $J_i(q^2)$. Ways to extract the latter from single or double differential angular distributions in $B \rightarrow K^*(\rightarrow K\pi)\mu^+\mu^-$ decays have been given in¹³.

^a Assuming standard model-type operators commonly termed \mathcal{O}_7 , \mathcal{O}_9 and \mathcal{O}_{10} .

Eq. (2) further limits the number of independent CP-asymmetries in $B \rightarrow K^* \mu^+ \mu^-$ decays to three, one related to the rate, $a_{\text{CP}}^{(1)}$, one related to A_{FB} , $a_{\text{CP}}^{(2)}$, or with a more favorable normalization related to $H_T^{(2,3)}$, $a_{\text{CP}}^{(3)}$, and one from meson mixing, $a_{\text{CP}}^{\text{mix}}$ ⁷.

Beylich *et al.* ¹⁴ recently proposed a local expansion without engaging heavy quark effective theory. In their OPE, Eq. (2) is not manifest, hence the aforementioned symmetry-based high- q^2 predictions 1. – 3. are no longer explicit, however, the OPE itself has a simpler structure. It will become most useful once all $B \rightarrow K^*$ form factors are known with sufficient accuracy.

The treatment of the high- q^2 region is based on an OPE, whose performance can be tested by checking *e.g.*, Eq. (3). The OPE is supported by consistency between the constraints obtained from excluding and using only the high- q^2 region data ⁶, and by a recent model-study ¹⁴.

2.2 Angular Distributions

With high event rates at the horizon the angular analysis with an on-shell decaying $K^* \rightarrow K \pi$ ¹⁵ has received recently a lot of attention as a tool to maximize the extraction of physics from $B \rightarrow K^* \mu^+ \mu^-$ decays ^{6,7,13,16,17,18}. In a full angular analysis the quartic differential decay distribution $d^4\Gamma$ factorizes into q^2 -dependent angular coefficients J_i and trigonometric functions of three angles: θ_l , the angle between the l^- and the \bar{B} in the dilepton CMS, θ_{K^*} , the angle between the K and the \bar{B} in the K^* -CMS and ϕ , the angle between the normals of the $K\pi$ and l^+l^- plane

$$d^4\Gamma = \frac{3}{8\pi} J(q^2, \theta_l, \theta_{K^*}, \phi) dq^2 d\cos\theta_l d\cos\theta_{K^*} d\phi, \quad (7)$$

where

$$\begin{aligned} J(q^2, \theta_l, \theta_{K^*}, \phi) &= J_1^s \sin^2 \theta_{K^*} + J_1^c \cos^2 \theta_{K^*} + (J_2^s \sin^2 \theta_{K^*} + J_2^c \cos^2 \theta_{K^*}) \cos 2\theta_l \\ &+ J_3 \sin^2 \theta_{K^*} \sin^2 \theta_l \cos 2\phi + J_4 \sin 2\theta_{K^*} \sin 2\theta_l \cos \phi + J_5 \sin 2\theta_{K^*} \sin \theta_l \cos \phi \\ &+ J_6 \sin^2 \theta_{K^*} \cos \theta_l + J_7 \sin 2\theta_{K^*} \sin \theta_l \sin \phi \\ &+ J_8 \sin 2\theta_{K^*} \sin 2\theta_l \sin \phi + J_9 \sin^2 \theta_{K^*} \sin^2 \theta_l \sin 2\phi, \quad J_i = J_i(q^2). \end{aligned} \quad (8)$$

The angular analysis offers opportunities for searches for beyond the standard model (BSM) CP-violation. The angular distribution $d^4\bar{\Gamma}$ of the CP-conjugate decays is obtained from $d^4\Gamma$ after flipping the sign of the CP phases and by replacing $J_{1,2,3,4,7} \rightarrow \bar{J}_{1,2,3,4,7}$ and $J_{5,6,8,9} \rightarrow -\bar{J}_{5,6,8,9}$. Several CP-asymmetries $A_i \propto J_i - \bar{J}_i$ can be obtained. Highlights include ^{7,13}: $A_{3,9}$ vanish in the standard model by helicity conservation, hence, they are sensitive to right-handed currents. $A_{3,9,(6)}$ can be extracted from a single-differential distribution in $\phi(\theta_l)$. $A_{7,8,9}$ are (naive) T -odd and not suppressed by small strong phases; they can be order one with order one BSM CP-phases. $A_{5,6,8,9}$ and $a_{\text{CP}}^{(3)}$ are CP-odd and can be extracted without tagging from $\Gamma + \bar{\Gamma}$; this is advantageous for $B_s, \bar{B}_s \rightarrow (\Phi \rightarrow K^+ K^-) \mu^+ \mu^-$ decays which are not self-tagging; time-integrated measurements are possible as well. Note that in the standard model all $b \rightarrow s$ CP-asymmetries are doubly Cabibbo-suppressed and small. At high q^2 , due to Eq. (2), $A_{7,8,9} = 0$. The angular distribution in $B \rightarrow K \mu^+ \mu^-$ decays involves only one angle θ_l and is simpler ¹⁹.

3 BSM Implications

Measurements of $B \rightarrow K^* \mu^+ \mu^-$ observables place model-independent constraints on the Wilson coefficients of the four-fermi operators $\mathcal{O}_{9,10}$. Assuming real-valued coefficients C_9, C_{10} the constraints from branching ratio and A_{FB} spectra at high q^2 are illustrated in the left-handed plot of Figure 2. The high- q^2 constraints from $A_{\text{FB}} \sim \text{Re}(C_{10} C_9^*)$ are orthogonal to the ones from the branching ratio $\sim |C_9|^2 + |C_{10}|^2$. The magnitude of C_7 is fixed by the measured $B \rightarrow X_s \gamma$ branching ratio to be near its standard model value.

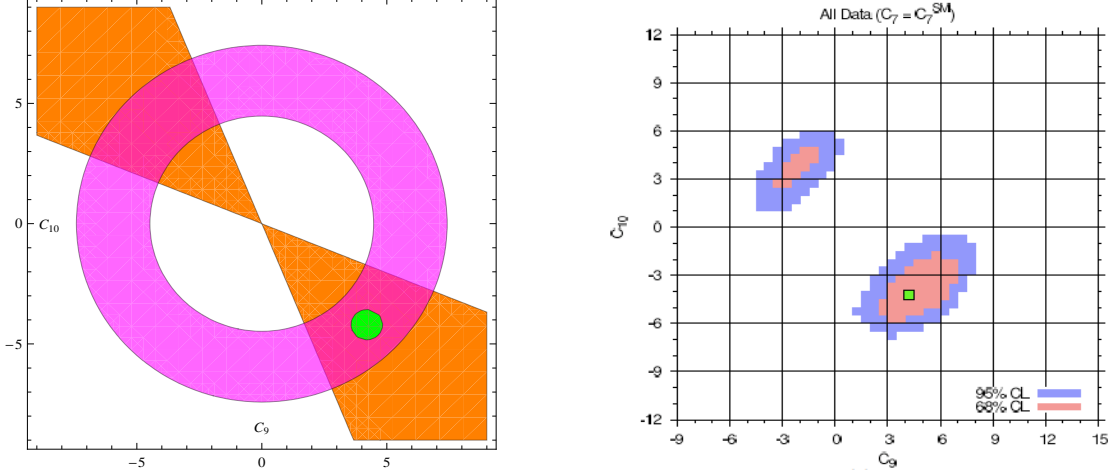


Figure 2: Today's model-independent bounds on real-valued C_9, C_{10} from $b \rightarrow s\mu^+\mu^-$ decays for $C_7 \simeq C_7^{\text{SM}} < 0$. The left-handed plot is schematic only and illustrates the allowed regions from branching ratio measurements (magenta ring) and A_{FB} determinations at large q^2 (orange wedges). The green dot corresponds to $(C_9^{\text{SM}}, C_{10}^{\text{SM}})$. The right-handed plot with the allowed 68 and 95 % C.L. regions is taken from Ref. [6]. There are similar plots for $C_7 \simeq -C_7^{\text{SM}} > 0$, hence in total four disconnected allowed regions in C_7, C_9 and C_{10} .

The outcome of a recent analysis using $B \rightarrow K^*\mu^+\mu^-$ data^{3,4,5} as well as the constraints from $B \rightarrow X_sl^+l^-$ decays is shown in the right-handed plot of Figure 2⁶. The constraints from A_{FB} at high q^2 significantly improve the scan. They are manifest in the plane by selecting arcs from the area allowed by the various branching ratio measurements. Because of the $\text{Re}(C_7C_9)$ interference term in $\mathcal{B}(B \rightarrow X_sl^+l^-)$ the ambiguity in the disconnected allowed regions is mildly broken. The allowed regions include the standard model, but order one deviations in all three Wilson coefficients C_7, C_9 and C_{10} are allowed as well.

The experimental situation of A_{FB} at low q^2 , unlike the one at high q^2 , is currently not settled, see Figure 1. To find out whether there is a zero-crossing of the A_{FB} at low q^2 as predicted by the standard model $q_0^2|_{\text{SM}} = 4.36_{-0.31}^{+0.33} \text{ GeV}^2$ (for $B^0 \rightarrow K^{*0}\mu^+\mu^-$), $q_0^2|_{\text{SM}} = 4.15 \pm 0.27 \text{ GeV}^2$ (for $B^+ \rightarrow K^{*+}\mu^+\mu^-$)¹⁰ and likewise for $B \rightarrow X_sl^+l^-$ decays $q_0^2|_{\text{SM}} = (3.34 \dots 3.40)_{-0.25}^{+0.22} \text{ GeV}^2$ ²¹ remains a central goal for next years b -physics programs.

A future analysis assuming the existence and determination of the A_{FB} zero at low q^2 is given in Figure 3. The establishment of the zero reduces the four-fold ambiguity to two. Resolving the last ambiguity requires precision studies sensitive to the contributions from four-quark operators which are commonly absorbed in the effective coefficients C_i^{eff} . Assuming vanishing or very small CP phases a lower bound on the position of the $A_{\text{FB}}(B \rightarrow K^*\mu^+\mu^-)$ zero can be derived from the respective upper bounds on $|C_9|$ ⁶. Very roughly, $q_0^2 \simeq q_0^2|_{\text{SM}}|C_9^{\text{SM}}|/|C_9^{\text{max}}| \gtrsim 2 \text{ GeV}^2$.

Model-independent $\Delta B = 1$ BSM implications can be drawn using an effective theory^b

$$\mathcal{H}_{\text{eff}} = \sum_i \frac{\tilde{c}_i}{\Lambda_{\text{NP}}^2} \tilde{O}_i, \quad \tilde{O}_{10} = \bar{s}\gamma_\mu(1 - \gamma_5)b \bar{\mu}\gamma^\mu\gamma_5\mu. \quad (9)$$

Assuming new physics at the scale $\Lambda_{\text{NP}} = 1 \text{ TeV}$ the coefficient of the higher dimensional operator \tilde{O}_{10} needs a (flavor) suppression as strong as $|\tilde{c}_{10}| < 2 \cdot 10^{-3}$ ($5 \cdot 10^{-3}$). If one assumes no suppression at all, $|\tilde{c}_{10}| = 1$, the scale of new physics is pushed up to

$$\Lambda_{\text{NP}} > 26 \text{ TeV} \text{ (15 TeV)}. \quad (10)$$

The bounds are obtained at 95 % C.L.⁶. The first numbers correspond to $\max|C_{10} - C_{10}^{\text{SM}}|$ from the nearby solution, that is, from the allowed region including the standard model whereas

^bThanks to Gilad Perez for suggesting this.

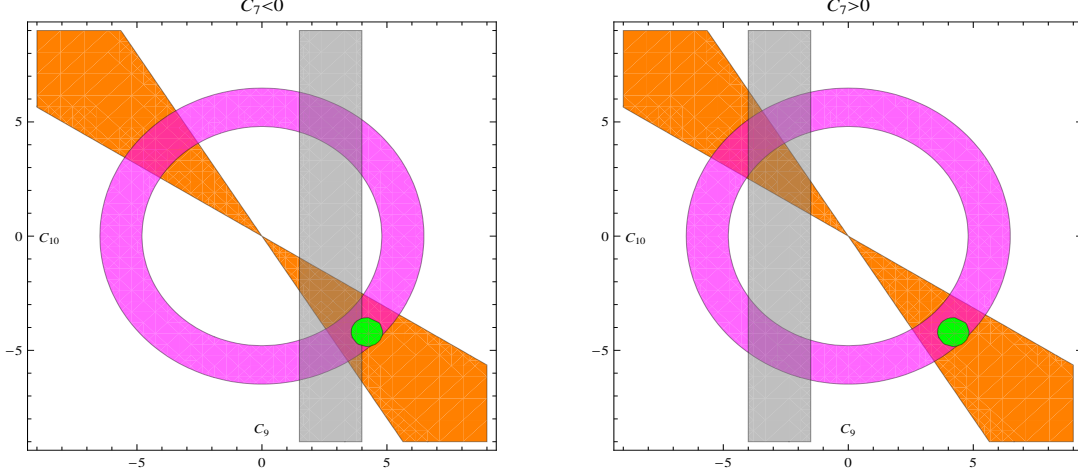


Figure 3: Future scenario of the model-independent bounds on real-valued C_9, C_{10} from $b \rightarrow s\mu^+\mu^-$ decays for $C_7 \simeq C_7^{\text{SM}} < 0$ (left-handed plot) and $C_7 \simeq -C_7^{\text{SM}} > 0$ (right-handed plot). The grey vertical bands denote the constraints arising if an A_{FB} zero at low q^2 could be established. There remain two allowed disconnected regions.

the weaker bounds in parentheses are obtained from the far away region, not connected to $(C_9^{\text{SM}}, C_{10}^{\text{SM}})$.

A recent complex-valued scan²² in $C_{7,9,10}$ returns the allowed 68% C.L. (95% C.L.) ranges⁷

$$\begin{aligned} 0.8 \leq |C_9| \leq 6.8 \quad (0.0 \leq |C_9| \leq 7.8), \\ 1.8 \leq |C_{10}| \leq 5.5 \quad (0.8 \leq |C_{10}| \leq 6.3). \end{aligned} \quad (11)$$

with some of the lower bounds being sensitive to the discretization of the scan. The constraints on the CP phases are not very strong, approximately $\frac{\pi}{2} \lesssim \arg(C_9 C_{10}^*) \lesssim \frac{3\pi}{2}$ at 68% C.L.⁷.

Eqs. (11) imply a maximal enhancement of the $\bar{B}_s \rightarrow \mu^+\mu^-$ branching ratio $\mathcal{B}(\bar{B}_s \rightarrow \mu^+\mu^-) \propto f_{\bar{B}_s}^2 |C_{10}|^2$ with respect to its standard model value by a factor 2.3. The dominant uncertainty of the standard model prediction is stemming from the decay constant of the B_s meson. Using^{23 24} gives⁷

$$\begin{aligned} \mathcal{B}(\bar{B}_s \rightarrow \mu^+\mu^-)_{\text{SM}} &= (3.1 \pm 0.6) \times 10^{-9}, \quad f_{B_s} = 231(15)(4) \text{ MeV} \quad (\text{Gamiz et al '09}), \\ \mathcal{B}(\bar{B}_s \rightarrow \mu^+\mu^-)_{\text{SM}} &= (3.8 \pm 0.4) \times 10^{-9}, \quad f_{B_s} = 256(6)(6) \text{ MeV} \quad (\text{Simone et al '10}). \end{aligned} \quad (12)$$

It follows the upper limit (at 95 % C.L.)⁷

$$\mathcal{B}(\bar{B}_s \rightarrow \mu^+\mu^-) < 10 \times 10^{-9}, \quad (13)$$

which could be invalidated by sizable contributions from scalar and pseudo-scalar operators not considered here. Experimentally, $\mathcal{B}(\bar{B}_s \rightarrow \mu^+\mu^-) < 43 \times 10^{-9}$ at 95 % C.L. from CDF²⁵.

4 Outlook

At this stage first results for basic decay distributions and asymmetries of exclusive $b \rightarrow sl^+l^-$ modes have become available. With more data soon and shrinking error bars the constraints from the $\Delta B = 1$ analysis will tighten. Steep progress in the BSM reach is expected from additional and complementary observables which could remove – or verify – currently allowed solutions far away from the standard model. A useful nearer term observable in this regard is A_{FB} at low recoil, perhaps also combined with improved constraints from the $B \rightarrow X_s l^+l^-$ branching ratio. Further observables designed with good theory properties are accessible by angular analysis, which is promising for higher statistics searches.

BSM models often induce operators beyond those of the standard model. These include right-handed currents, enhanced scalar and pseudo-scalar couplings or lepton-flavor non-universal effects, and can *e.g.* be searched for with, respectively, transverse asymmetries¹⁶, $\bar{B}_s \rightarrow \mu^+ \mu^-$ or by comparing $l = e$ to μ modes¹⁹. $\mathcal{O}(1)$ BSM CP phases can show up as $\mathcal{O}(1)$ T -odd CP asymmetries $A_{7,8,9}$ ¹³. Angular analysis becomes most powerful and essential here.

Dimuons provide great opportunities for LHC(b) and the Tevatron. They could also be studied at future super flavor e^+e^- factories, which moreover have good capabilities to investigate dielectron and inclusive modes, and missing energy searches covering $l = \nu$ or possibly $l = \tau$.

Acknowledgments

GH is happy to thank her collaborators from the EOS team and the organizers of the 2011 Moriond Electroweak session for the invitation to the meeting. The works presented here are supported in part by the Bundesministerium für Bildung und Forschung (BMBF).

1. A. Ali, P. Ball, L. T. Handoko and G. Hiller, Phys. Rev. D **61**, 074024 (2000), [arXiv:hep-ph/9910221].
2. C. Bobeth, G. Hiller and G. Piranishvili, PoS **BEAUTY2009**, 047 (2009) [arXiv:0911.4054 [hep-ph]].
3. B. Aubert *et al.* [BABAR Collaboration], Phys. Rev. Lett. **102**, 091803 (2009), [arXiv:0807.4119 [hep-ex]].
4. J. T. Wei *et al.* [BELLE Collaboration], Phys. Rev. Lett. **103**, 171801 (2009), [arXiv:0904.0770 [hep-ex]].
5. T. Aaltonen *et al.* [CDF Collaboration], arXiv:1101.1028 [hep-ex].
6. C. Bobeth, G. Hiller and D. van Dyk, JHEP **1007**, 098 (2010), [arXiv:1006.5013 [hep-ph]].
7. C. Bobeth, G. Hiller and D. van Dyk, arXiv:1105.0376 [hep-ph].
8. A. Golutvin for the LHCb collaboration; Talk given at La Thuile 2011.
9. B. Grinstein and D. Pirjol, Phys. Rev. D **70**, 114005 (2004), [arXiv:hep-ph/0404250].
10. M. Beneke, T. Feldmann, D. Seidel, Eur. Phys. J. **C41**, 173-188 (2005), [hep-ph/0412400].
11. A. Khodjamirian, T. Mannel, A.A. Pivovarov and Y.M. Wang, JHEP **1009** (2010) 089, [arXiv:1006.4945 [hep-ph]].
12. B. Grinstein and D. Pirjol, Phys. Lett. B **533**, 8 (2002), [arXiv:hep-ph/0201298].
13. C. Bobeth, G. Hiller and G. Piranishvili, JHEP **0807**, 106 (2008), [arXiv:0805.2525 [hep-ph]].
14. M. Beylich, G. Buchalla and T. Feldmann, arXiv:1101.5118 [hep-ph].
15. F. Kruger, L. M. Sehgal, N. Sinha and R. Sinha, Phys. Rev. D **61**, 114028 (2000) [Erratum-ibid. D **63**, 019901 (2001)], [arXiv:hep-ph/9907386].
16. U. Egede *et al.*, JHEP **0811**, 032 (2008), [arXiv:0807.2589 [hep-ph]].
17. W. Altmannshofer *et al.*, JHEP **0901**, 019 (2009), [arXiv:0811.1214 [hep-ph]].
18. U. Egede, T. Hurth, J. Matias *et al.*, JHEP **1010**, 056 (2010), [arXiv:1005.0571 [hep-ph]].
19. C. Bobeth, G. Hiller, G. Piranishvili, JHEP **0712**, 040 (2007). [arXiv:0709.4174 [hep-ph]].
20. Z. Liu *et al.*, arXiv:1101.2726 [hep-ph].
21. G. Bell, M. Beneke, T. Huber, X. -Q. Li, Nucl. Phys. **B843**, 143-176 (2011). [arXiv:1007.3758 [hep-ph]].
22. D. van Dyk *et al.*, Online <http://project.het/source/eos/>.
23. E. Gamiz, C. T. H. Davies, G. P. Lepage, J. Shigemitsu and M. Wingate [HPQCD Collaboration], Phys. Rev. D **80** (2009) 014503, [arXiv:0902.1815 [hep-lat]].
24. J. Simone *et al.* [Fermilab Lattice and MILC Collaborations], PoS **LATTICE2010** (2010) 317.
25. CDF Public Note 9892; with 3.7 fb^{-1} .